Biophysical Letter

Force-Induced Unfolding of Leucine-Rich Repeats of Glycoprotein Ibα Strengthens Ligand Interaction

Lining Ju,[1,3,4,5,*] Jizhong Lou,[6] Yunfeng Chen,[2,3] Zhenhai Li,[7] and Cheng Zhu[1,2,3,*]

[1]Coulter Department of Biomedical Engineering, [2]Woodruff School of Mechanical Engineering, and [3]Petit Institute for Bioengineering and Biosciences, Georgia Institute of Technology, Atlanta, Georgia; [4]Heart Research Institute and [5]Charles Perkins Centre, The University of Sydney, Camperdown, New South Wales, Australia; [6]Laboratory of RNA Biology, Institute of Biophysics, Chinese Academy of Sciences, Beijing, China; and [7]Quantum Beam Science Directorate, Japan Atomic Energy Agency, Kizugawa, Kyoto, Japan

ABSTRACT Leucine-rich repeat (LRR) is a versatile motif widely present in adhesive proteins and signal-transducing receptors. The concave structure formed by a group of LRRs is thought to facilitate binding to globular protein domains with increased affinities. However, little is known about the conformational dynamics of LRRs in such a structure, e.g., whether and how force induces conformational changes in LRRs to regulate protein binding and signal transduction. Here we investigated the platelet glycoprotein Ibα (GPIbα), a demonstrated mechanoreceptor with known crystal structures for the N-terminal domain (GPIbαN), as a model for LRR-containing proteins using a combined method of steered molecular dynamics simulations and single-molecule force spectroscopy with a biomembrane force probe. We found that force-induced unfolding of GPIbαN starts with LRR2–4 and propagates to other LRRs. Importantly, force-dependent lifetimes of individual VWF-A1 bonds with GPIbα are prolonged after LRR unfolding. Enhancement of protein-protein interactions by force-induced LRR unfolding may be a phenomenon of interest in biology.

Received for publication 12 February 2015 and in final form 24 August 2015.

*Correspondence: arnold.ju@sydney.edu.au or cheng.zhu@bme.gatech.edu

Binding of von Willebrand factor (VWF) to platelet membrane receptor glycoprotein Ibα (GPIbα) initiates hemostasis and thrombosis under high shear conditions, mostly seen in arteries and restricted vessels (1). VWF is a multimeric protein composed of identical 250-kDa subunits. Each subunit has a single 24-kDa A1 domain that binds to the 45 kDa, ~280 residues, N-terminal domain of GPIbα (GPIbαN). The crystal structures of the A1-GPIbαN complex (2,3) reveal that GPIbαN consists of eight leucine-rich repeats (LRRs, K19–L208) that form an elongated shape (cf. Fig. 1 *A*). The concave LRR framework grabs the A1 in a pincerlike grip with an N-terminal contact (involving the β-finger motif and LRR1) and a C-terminal contact (involving LRR5–8 and the β-switch loop). Intriguingly, the middle portion of the GPIbαN, from LRR2–4, makes no contacts to the A1 in the crystal structures; yet, these LRRs are required for ristocetin-dependent and shear dependent VWF binding (4). Because crystal structures were obtained in the absence of force, they provide little insight into any possible conformational change induced by shear.

Single-molecule force spectroscopic studies using atomic force microscopy, an optical trap, and a biomembrane force probe (BFP) suggested that at least two conformational states may exist upon formation of the receptor-ligand complex (5). A recent crystal structure of a gain-of-function mutant A1 complexed with GPIbαN revealed A1 interaction with LRR3-5 that further enhances the A1-GPIbαN affinity (6). These findings suggest that force may induce a conformational change that alters the central A1-GPIbα LRR contact to enhance affinity.

Force induces LRR conformational change on A1-GPIbα bond in simulations

To investigate whether the force applied on the A1-GPIbα complex can cause significant protein conformational change, we carried out 11 independent steered molecular dynamics (SMD) simulations and observed in four trajectories unfolding of GPIbαN before dissociation from A1. At the starting point ($t = 0$), GPIbαN contacts A1 via the β-switch and β-finger (Fig. 1 *A*). At $t > 0$, the Cα atom of GPIbαN C-terminal residue L267 was pulled to move horizontally at a constant speed to the right with the Cα atom of the A1 N-terminal residue H1268 harmonically constrained. Upon loosening of the β-switch from the A1 central β-sheet at 9 ns (Fig. 1 *B*), the GPIbαN started to tilt about the β-finger–A1 hinge point, a counterclockwise rotation that continued throughout the remainder of the simulations. At 10 ns, the GPIbα β-switch

Editor: Nathan Baker.

http://dx.doi.org/10.1016/j.bpj.2015.08.050

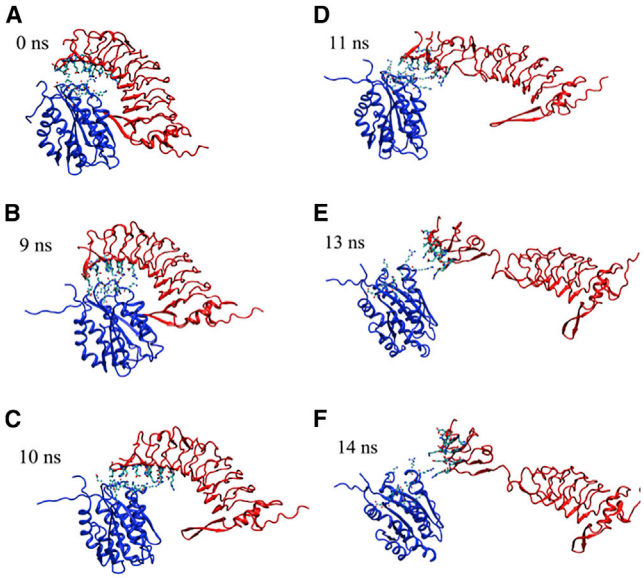

FIGURE 1 SMD simulation of GPIbαN dissociation from the A1 domain. Sequential snapshots of representative SMD-simulated structures revealing that force induces GPIbαN unfolding in the middle region of GPIbαN (LRR2–4). (*Blue*, A1; *red*, GPIbαN.) The equilibrated structure (*A*) was used as the starting structure for SMD simulations, which generated the structures in (*B*)–(*F*) at the indicated times. To see this figure in color, go online.

dissociated from the A1 central β-sheet, but the β-finger remained bound to A1, although interacting with different A1 residues from those seen at 0 ns (Fig. 1 *C*). At 11 ns, several hydrophobic interactions near the GPIbαN β-finger were ruptured by further pulling (Fig. 1 *D*). Surprisingly, a few residues spanning the LRR3, T68–L89, uncoupled from each other and became loose. At 12 ns, the LRR3 was completely unfolded and extended by force (Fig. 1 *E*). At 14 ns, the region below LRR3, e.g., LRR4, started getting loose; however, the GPIbαN dissociated from A1 before complete unfolding of LRR4 was observed (Fig. 1 *F*). Additional simulations with different force loading rates and anchor points showed similar LRR unfolding behavior (Fig. S1 in the Supporting Material). Regardless of the anchor point, GPIbαN unfolding started at LRR2-3 in a fast pulling process, suggesting that rapid loading facilitates LRR extension (Fig. S1, *B* and *C*).

Experimental characterization of force-induced conformational change in individual A1-GPIbα complexes

We next used the previously described BFP force spectroscopy (7,13) to observe conformational change in single A1-GPIbα complexes and its impact on force-dependent bond lifetimes (Fig. 2, *A* and *B*). In the BFP force traces, a sudden force drop occurring at 5–20 pN, caused by an abrupt length increase between the probe and the target, was consistently (~14% occurrence) observed in the retraction phase when a ramp force (1000 pN/s) was applied to the extracellular portion of GPIba, glycocalicin (GC), via A1 (Fig. 2, *C* and *E*). Pulling GC via a monoclonal antibody (mAb) HIP1 yielded a similar unfolding occurrence as pulling via A1 (Fig. 2 *E*). In contrast, unfolding event was eliminated when HIP1 was replaced by another mAb SZ2 on the probe or when GC was replaced by an anti-A1 mAb 5D2 on the target (Fig. 2, *D* and *E*). This indicates that it was GC, not A1, that was being unfolded, and that unfolding occurred within the LRR region, because the binding epitope of SZ2 is mapped to the anionic region below all LRR domains (8) (Fig. 2 *G*).

The force-extension analysis showed that the extension lengths range from the minimum of 18 nm (l_{min} = length of one LRR, assuming a contour length of 4 Å per residue) to the maximum of 56 nm (l_{max} = length of six LRRs) (Fig. 2, *F* and *G*). Surprisingly, the A1–GC unfolding length histogram right-shifted when force loading rate was increased from 1000 to 3000 pN/s (Fig. 2 *F*). The unfolding length difference between the l_{max}(3000 pN/s) (= 69 nm, i.e., LRR2-8) and l_{max}(1000 pN/s) (= 56 nm, i.e., LRR3–8) is ~13 nm (Fig. 2 *G*), matching the length difference (~11 nm) between the unfolding starting points (LRR2 to LRR3) by different SMD ramping processes (Fig. S1). The combined SMD simulations (Figs. 1 and S1) and the BFP results indicated that force can unfold multiple repeats of the LRR region starting from the noncontact LRR2-4.

To investigate the functional consequence of the force-induced GPIbα unfolding, we measured lifetimes of A1 bonds with GC on a bead (Fig. 3 *A*) or GPIbα on a platelet (Fig. 3 *B*). Consistent with our previous reports (7,9,13), force counterintuitively prolongs bond lifetime (catch bond) from 10 to 25 pN. Further increase in force reduces bond lifetime (slip bond). To delineate the role of force-induced unfolding, we segregated the lifetimes into two subgroups based on whether an unfolding event was observed in the force-ramp phase (Fig. 2 *C*). In >20 pN forces, however, bond lifetimes with unfolding events became longer than those without unfolding events (Fig. 3, *A* and *B*). This indicates that GPIbα unfolding can immediately prolong the lifetime of its bond with VWF-A1.

Most studies on the effect of force on the structure of the VWF-GPIbα axis focus on shear-induced conformational changes in the VWF. As a long molecule (>40 nm above the membrane) (10), however, GPIbα may also appear susceptible to the conformational change upon force application. A recent study identified a mechanosensitive domain in the juxtamembrane region below the GC portion that can be unfolded by pulling force (11). The authors suggest that no other GPIbα region can be unfolded, as mutations in this mechanosensitive domain abolished the force-induced unfolding they observed.

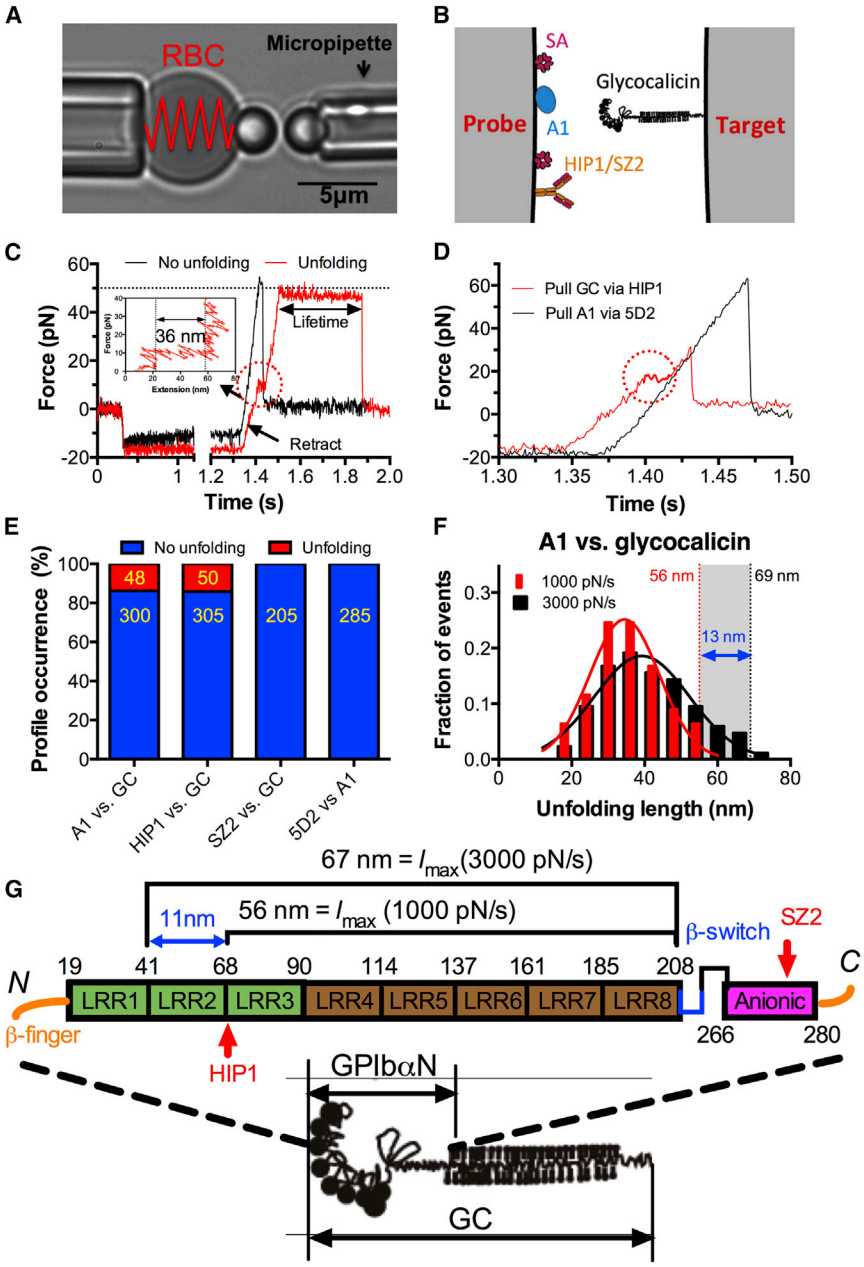

FIGURE 2 GPIbαN unfolding observed by BFP force-clamp assay. (*A*) BFP photomicrograph. A micropipette-aspirated RBC with a bead (*left*, probe) attached to the apex formed a picoforce sensor. It was aligned with another bead (*right*, target) aspirated by an apposing micropipette. (*B*) BFP functionalization with indicated molecules. (*C* and *D*) Force versus time traces from representative force-clamp cycles for A1-GC bond lifetime measurement (*C*) and antibody-protein stretch assay (*D*). (*Inset*) The putative unfolding event is circled and zoomed-in to show the details. (*E*) Occurrence frequencies of unfolding-versus-no-unfolding events (numbers are indicated in *yellow*) from all binding events mediated by the indicated interactions. (*F*) Normalized histograms (*bar*) and their Gaussian fits of unfolding length. (*G*) Glycocalicin schematic (*left*) and GPIbαN domain organization (*right*). Starting and ending residues for each domain as well as the binding epitopes of two anti-GPIbα mAbs are all indicated. To see this figure in color, go online.

Here we show GPIbαN conformational changes that enhance binding to VWF-A1, indicating the functional relevance of the LRR unfolding. Our results suggest that force extends the GPIbαN concave structure by unfolding a few LRRs, allowing the globular A1 domain to fit better into the enlarged binding pocket and reach a longer-lived state (Fig. 3 *C*). This may explain platelets agglutination via VWF-GPIbα bonds without activation or binding of integrin GPIIb/IIIa at sites of atherothrombosis where severe vessel narrowing produces extremely high shears (>10,000 s^{-1}) (12). Whether GPIbα mechanosensitivity endows this molecule with the capacity of mechanosensing requires future studies.

SUPPORTING MATERIAL

Supporting Materials and Methods and one figure are available at http://www.biophysj.org/biophysj/supplemental/S0006-3495(15)00946-7.

AUTHOR CONTRIBUTIONS

L.J. and C.Z. designed experiments; L.J., J.L., Y.C., and Z.L. performed experiments and analyzed the data; and all authors contributed to writing.

ACKNOWLEDGMENTS

We thank Renhao Li and the Emory blood bank for providing outdated platelets, and Jing-fei Dong and Vince F. Fiore for purifying glycocalicin.

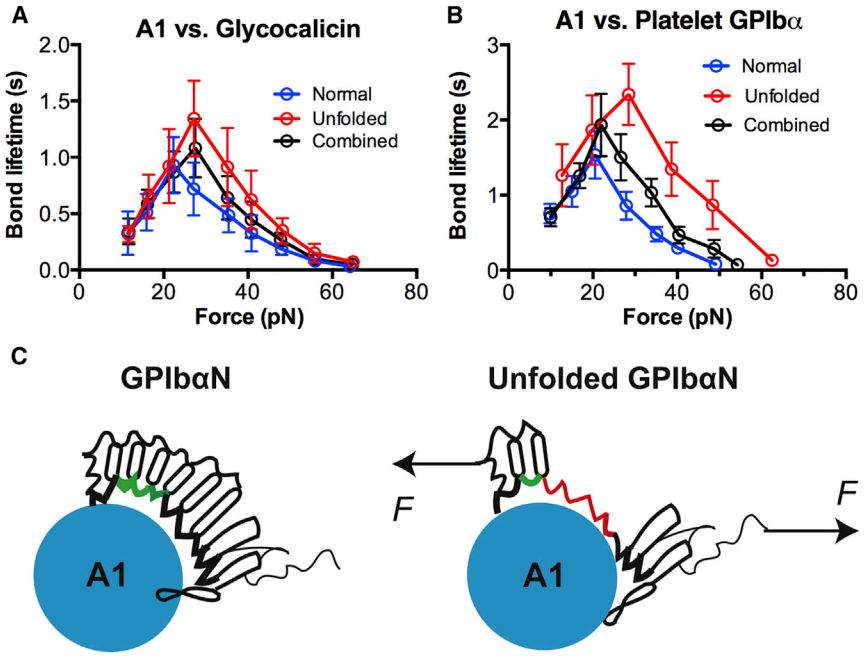

FIGURE 3 Unfolding of GPIbαN prolongs the bond lifetime. (*A* and *B*) Plots of lifetime (mean ± SE of >20 measurements per point) versus force of VWF-A1 bonds with GC (*A*) or GPIbα on platelets (*B*). (*C*) Schematic of the A1-GPIbαN complex in normal state (*left*) and force, induced a longer-lived state (*right*). (*Horizontal arrows*) Tensile forces. To see this figure in color, go online.

This work was supported by National Institutes of Health grants No. HL091020 and No. HLR01HL093723 (to C.Z.).

REFERENCES

1. Gardiner, E. E., and R. K. Andrews. 2014. Structure and function of platelet receptors initiating blood clotting. *Adv. Exp. Med. Biol.* 844:263–275.
2. Huizinga, E. G., S. Tsuji, …, P. Gros. 2002. Structures of glycoprotein Ibα and its complex with von Willebrand factor A1 domain. *Science.* 297:1176–1179.
3. Dumas, J. J., R. Kumar, …, L. Mosyak. 2004. Crystal structure of the wild-type von Willebrand factor A1-glycoprotein Ibα complex reveals conformation differences with a complex bearing von Willebrand disease mutations. *J. Biol. Chem.* 279:23327–23334.
4. Shen, Y., S. L. Cranmer, …, R. K. Andrews. 2006. Leucine-rich repeats 2–4 (Leu^{60}-Glu^{128}) of platelet glycoprotein Ibα regulate shear-dependent cell adhesion to von Willebrand factor. *J. Biol. Chem.* 281: 26419–26423.
5. Liu, B., W. Chen, and C. Zhu. 2015. Molecular force spectroscopy on cells. *Annu. Rev. Phys. Chem.* 66:427–451.
6. Blenner, M. A., X. Dong, and T. A. Springer. 2014. Towards the structural basis of regulation of von Willebrand factor binding to glycoprotein Ib. *J. Biol. Chem.* 289:5565–5579.
7. Ju, L., J.-F. Dong, …, C. Zhu. 2013. The N-terminal flanking region of the A1 domain regulates the force-dependent binding of von Willebrand factor to platelet glycoprotein Ibα. *J. Biol. Chem.* 288:32289–32301.
8. Shen, Y., G. M. Romo, …, R. K. Andrews. 2000. Requirement of leucine-rich repeats of glycoprotein (GP) Ibα for shear-dependent and static binding of von Willebrand factor to the platelet membrane GP Ib-IX-V complex. *Blood.* 95:903–910.
9. Yago, T., J. Lou, …, C. Zhu. 2008. Platelet glycoprotein Ibα forms catch bonds with human WT vWF but not with type 2B von Willebrand disease vWF. *J. Clin. Invest.* 118:3195–3207.
10. Fox, J. E., L. P. Aggerbeck, and M. C. Berndt. 1988. Structure of the glycoprotein Ib•IX complex from platelet membranes. *J. Biol. Chem.* 263:4882–4890.
11. Zhang, W., W. Deng, …, R. Li. 2015. Identification of a juxtamembrane mechanosensitive domain in the platelet mechanosensor glycoprotein Ib-IX complex. *Blood.* 125:562–569.
12. Ruggeri, Z. M., J. N. Orje, …, A. J. Reininger. 2006. Activation-independent platelet adhesion and aggregation under elevated shear stress. *Blood.* 108:1903–1910.
13. Ju, L., Y. Chen, …, M. A. Cruz. 2015. Von Willebrand factor-A1 domain binds platelet glycoprotein Ibα in multiple states with distinctive force-dependent dissociation kinetics. *Thromb. Res.* 136:606–612.

Supporting Materials for

Force-Induced Unfolding of Leucine-Rich Repeats of Glycoprotein Ibα Strengthens Ligand Interaction

Lining Ju,[1,3,4,5,*] Jizhong Lou,[6] Yunfeng Chen,[2,3] Zhenhai Li,[7] and Cheng Zhu[1,2,3,*]

[1]Coulter Department of Biomedical Engineering, [2]Woodruff School of Mechanical Engineering, and [3]Petit Institute for Bioengineering and Biosciences, Georgia Institute of Technology, Atlanta, Georgia; [4]Heart Research Institute and [5]Charles Perkins Centre, The University of Sydney, Camperdown, New South Wales, Australia; [6]Laboratory of RNA Biology, Institute of Biophysics, Chinese Academy of Sciences, Beijing, China; and [7]Quantum Beam Science Directorate, Japan Atomic Energy Agency, Kizugawa, Kyoto, Japan

Supplementary Figure S1

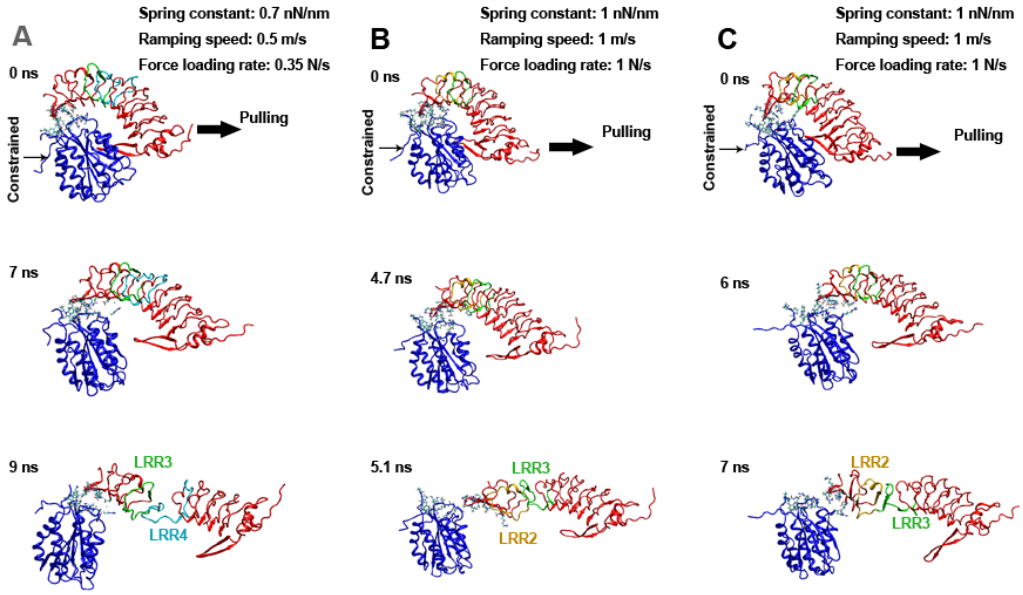

Supplementary Figure S1, corresponding to Fig. 1. Sequential snapshots of three SMD simulations of GPIbαN dissociation from the A1 domain under different conditions. Upper, middle, and lower panels in each row represent, respectively, the moment when simulation began, GPIbαN (red) β-switch dissociated from the A1 (blue) central β-sheet, and LRRs unfolded. The constrained atom in A1 was either the residue C1272, Cα (A and C), or the residue H1268, C12 (B). The ramping speed was 0.7 m/s (A) or 1 m/s (B and C). The force loading point and pulling direction are indicated.

Materials and methods

SMD simulations.

SMD simulations were performed using the NAMD program with the CHARMM22 all-atom force field for protein as previously described (1). Briefly, The X-ray crystal structure of the A1–GPIbαN complex (Protein Data Bank code 1SQ0 (2)) was used as the initial structure, which was put in a 160 Å × 96 Å × 72 Å water box with 10 Na^+ and 21 Cl^- ions to neutralize the system, which contained 140,570 atoms. The system was subjected to 10,000 steps of energy minimization with heavy atoms fixed and another 10,000 steps with all atoms free. The system was heated gradually from 0-300K in 0.1 ns and then equilibrated for 3 ns with pressure and temperature control. The temperature was held at 300K using Langevin dynamics, and the pressure was held at 1 atm by the Langevin piston method. The equilibrated structure was taken as the starting point for SMD simulations. In SMD, the Cα atom of the A1 N-terminal residue H1268, C12 (Fig. 1 and Fig. S1B) or C1272, Cα (in Fig. S1A and C) was harmonically constrained and the Cα atom of the GPIbα C-terminal residue L267 was pulled at a constant ramping speed of 0.5 m/s (Fig. 1 and Fig. S1A) or 1 m/s (Fig. S1B and C) with spring constant of 0.7 nN/nm (Fig. 1 and Fig. S1A) or 1 nN/nm (Fig. S1B and C). We adjusted ramping speeds and spring constants in order to accelerate the processes, so that unbinding could be observed in 10–15 ns of the simulation time. Although the pulling speed used in MD simulations was several order of magnitude higher than those used in experiments and in blood flow, the results from MD simulations have been confirmed by force spectroscopy, suggesting the validity of MD simulations (3). Structures in Fig. 1 and S1 were generated using VMD (4).

Purification of platelets and red blood cells

Platelets and red blood cells (RBCs) were isolated from 3 ml venous blood drawn from healthy adult donors abiding the protocol approved by the Georgia Institute of Technology Institutional Review Board. Whole blood was first collected in a 1:10 ACD buffer (6.25 g sodium citrate, 3.1 g citric acid anhidrous, 3.4 g D-glucose in 250

ml H_2O, pH 6.7) and centrifuged at 150 g for 15 min at room temperature. Platelet-rich plasma (from the top yellow layer) was then centrifuged at 900 g for 5 min. The platelet pellet was gently resuspended in the HEPES-Tyrode buffer (134 mM NaCl, 12 mM NaHCO3, 2.9 mM KCl, 0.34 mM NaH_2PO_4, 5 mM HEPES, and 5 mM D-glucose, 1% Bovine serum albumin, pH 7.4) as the washed platelets (5). To avoid unwanted platelet activation by RBC released ADP, apyrase (0.01 U/mL) was added to the final platelet suspension.

RBCs (3 μl, from the bottom red layer) were resuspended in a carbonate/bicarbonate buffer (0.1M $NaHCO_3$ and Na_2CO_3, pH 8.5) and then biotinylated by covalently linking polymer biotin-PEG3500-SGA (JenKem USA, TX) with a 30 min incubation at room temperature (6). To balloon RBCs for the force probe use in the Tyrode buffer of physiological osmolarity, RBCs were further incubated with nystatin (Sigma-Aldrich) in an N2-5% buffer (265.2 mM KCl, 38.8 mM NaCl, 0.94 mM KH_2PO_4, 4.74 mM Na_2HPO_4, 27 mM sucrose; pH 7.2, 588 mOsm) for 30 min at 0°C. The modified RBCs were washed twice with the N2 buffer and resuspended in the N2 buffer for the BFP experiments (7).

Proteins and antibodies

Recombinant wild-type (WT) monomeric VWF-A1 (residues 1238-1471) generated by E.coli as previously described (5, 8) was a generous gift of Miguel A. Cruz (Baylor College of Medicine). Glycocalicin (GC, extracellular portion of GPIbα) was cleaved and purified from outdated platelets (Blood bank at Emory university) as described previously (9, 10). GC covers most of the GPIbα extracellular portion, consisting of the A1-binding domain GPIbαN and a long megaglycopipetide stalk (Fig. 2G). The GPIbαN zoom-in includes a N-terminal β-finger (residues 1-18, orange), eight LRRs (19–208, brown for repeats with A1 contacts and green for those without), a disulfide knot structure (209–265) including the C-terminal β-switch (227-240, blue), and a C-terminal anionic region (266–280, magenta) (Fig. 1). Two anti-GPIbα mAbs were purchased: HIP1(Abcam) and SZ2 (Santa Cruz Biotechnology). Anti-A1 mAb 5D2 was a gift from Dr. Michael Berndt (Curtin University, WA, Australia).

Functionalization of glass beads

Proteins (A1, GC and mAbs) were covalently modified with maleimide-PEG3500-NHS (MW ~3500 Da; JenKem, TX) in the carbonate/bicarbonate buffer. To coat maleimized proteins on glass beads, 2-μm (diameter) silanized borosilicatebeads (Thermo Scientific) were first covalently coupled with mercapto-propyl-trimethoxy silane (Sigma), followed by covalently linking to both streptavidin-maleimide (Sigma) and maleimide modified proteins in monobasic/dibasic phosphate buffer (0.2M NaH_2PO_4 and Na_2HPO_4, pH 6.8) (Fig. 2B, left). After overnight incubation and resuspending in phosphate buffer with 1% human serum albumin, beads were ready for immediate use in BFP experiments. The specificity and functional effect were justified in the previous study (5).

BFP experiments

Our BFP experimental procedure used to study VWF–GPIbα interaction has been described (5) with a default spring constant at 0.25 pN/nm. In each test cycle, the target (GC coated bead, Fig. 2A and B, right) was driven to approach and contact the probe (A1 or mAb coated bead, Fig. 2A and B, left) with an 18-pN compressive force for a certain contact time (1 s by default) to allow for bond formation and then was retracted at a preset ramping speed (4 μm/s by default) for adhesion detection. During the retraction, an adhesion event was signified by tensile force (>0 pN, Fig. 2C and D), but no tensile force (~0 pN) was detected in a no-adhesion event (13). The site density of either receptor or ligand was titrated low enough (<30/μm^2) on the contact area to achieve single-molecule level measurements with <20% adhesion frequency (11,13). To measure bond lifetime, the target was held at a desired clamp force (Fig. 2C, dotted line) to wait for bond dissociation and returned to the original position to complete the cycle. Lifetime was measured from the instant when the force reached the desired level to the instant of bond dissociation (Fig. 2C, red trace). To investigate the force loading rate effect (spring constant × ramping speed) on unfolding as

suggested by SMD simulations, we increased the spring constant to 3.75 pN/nm and the ramping speed to 8 μm/s (Fig. 2F) to match the respective 1.4 and 2 folds increases used in SMD (Fig. S1A vs. S1B,C). Therefore, we compared the different LRR unfolding behaviors between 1000 and 3000 pN/s force rates in experiments (Fig. 2F).

The molecular unfolding analysis was derived from a force versus extension curve (e.g., Fig. 2C inset), which was converted from force versus time data (e.g., Fig. 2C). Here, molecular extension was calculated as differential displacement between the BFP tracking system (probe positioning) and the piezoelectric actuator feedback system (target positioning) as previously described (12). The unfolding activity was signified by a sudden extension increase of >5 nm, whereas force remained or dropped. The extension length was considered as the unfolding contour length.

References:

1. Yago, T., J. Lou, T. Wu, J. Yang, J.J. Miner, et al. 2008. Platelet glycoprotein Ibalpha forms catch bonds with human WT vWF but not with type 2B von Willebrand disease vWF. J Clin Invest. 118: 3195–3207.

2. Dumas, J.J., R. Kumar, T. McDonagh, F. Sullivan, M.L. Stahl, et al. 2004. Crystal structure of the wild-type von Willebrand factor A1-glycoprotein Ibalpha complex reveals conformation differences with a complex bearing von Willebrand disease mutations. J Biol Chem. 279: 23327–23334.

3. Rico, F., L. Gonzalez, I. Casuso, M. Puig-Vidal, and S. Scheuring. 2013. High-speed force spectroscopy unfolds titin at the velocity of molecular dynamics simulations. Science. 342: 741–743.

4. Humphrey, W., A. Dalke, and K. Schulten. 1996. VMD: visual molecular dynamics. J Mol Graph. 14: 33–38.

5. Ju, L., J.-F. Dong, M.A. Cruz, and C. Zhu. 2013. The N-terminal flanking region of the A1 domain regulates the force-dependent binding of von Willebrand factor to platelet glycoprotein Ibα. J Biol Chem. 288: 32289–32301.

6. Evans, E., K. Ritchie, and R. Merkel. 1995. Sensitive force technique to probe molecular adhesion and structural linkages at biological interfaces. Biophys J. 68: 2580–2587.

7. Liu, B., W. Chen, B.D. Evavold, and C. Zhu. 2014. Accumulation of dynamic catch bonds between TCR and agonist peptide-MHC triggers T cell signaling. Cell. 157: 357–368.

8. Cruz, M.A., and R.I. Handin. 1993. The interaction of the von Willebrand factor-A1 domain with platelet glycoprotein Ib/IX. J Biol Chem. 268: 21238–21245.

9. Fox, J.E. 1985. Linkage of a membrane skeleton to integral membrane glycoproteins in human platelets. Identification of one of the glycoproteins as glycoprotein Ib. J Clin Invest. 76: 1673–1683.

10. Fox, J.E., L.P. Aggerbeck, and M.C. Berndt. 1988. Structure of the glycoprotein Ib.IX complex from platelet membranes. J Biol Chem. 263: 4882–4890.

11. Chen, W., V.I. Zarnitsyna, K.K. Sarangapani, J. Huang, and C. Zhu. 2008. Measuring Receptor–Ligand Binding Kinetics on Cell Surfaces: From Adhesion Frequency to Thermal Fluctuation Methods. Cel. Mol. Bioeng. 1: 276–288.

12. Chen, W., J. Lou, E.A. Evans, and C. Zhu. 2012. Observing force-regulated conformational changes and ligand dissociation from a single integrin on cells. J Cell Biol. 199: 497–512.

13. Ju, L., Y. Chen, F. Zhou, H. Lu, M.A. Cruz, et al. 2015. Von Willebrand factor-A1 domain binds platelet glycoprotein Ibα in multiple states with distinctive force-dependent dissociation kinetics. Thrombosis Research. 136: 606–612.